

Angular Distribution and Yield of the Process $p+d \rightarrow t+\pi^+$

WILSON J. FRANK, KENNETH C. BANDELT, RICHARD MADEY,* AND BURTON J. MOYER
Radiation Laboratory, Department of Physics, University of California, Berkeley, California

(Received February 23, 1954)

The angular distribution of the process $p+d \rightarrow t+\pi^+$ has been determined for 340-Mev incident protons from the Berkeley 184-inch synchrocyclotron. The process was identified at one angle by a comparison of measured values with predicted values of the correlated angles, particle ranges, and triton time of flight. During one continuous run differential cross sections were measured at six pion center-of-mass angles ranging from 30° to 150° , with the apparatus set for the predicted correlated angles, minimum ranges, and triton time flight but without further tests of identification. The cross section is constant at about 0.45 microbarns/steradian over pion center-of-mass angles of 180° to 90° . The cross section rises in the forward direction to a value around 5 microbarns/steradian at 0° . The total yield of the process is estimated by numerical integration to be 15 microbarns.

A COMPARISON of the process $p+d \rightarrow t+\pi^+$ and its partner process $p+d \rightarrow \text{He}^3+\pi^0$ would provide a stringent test^{1,2} of the charge-independence hypothesis. If nuclear interactions are charge-independent in this energy region, the angular distributions of these two processes should be identical, and the ratio of the total cross sections, or the differential cross sections at any center-of-mass angle, should be 2:1. As an exploratory experiment, the angular distribution of the process $p+d \rightarrow t+\pi^+$ was measured.

This process, however, is of interest for its own sake, since its relation to the analogous process $p+p \rightarrow d+\pi^+$ makes it amenable to theoretical treatment. A prediction^{1,3} of its angular distribution and yield involves some assumptions about the deuteron and triton wave functions and an estimate of the angular distribution and yield of the process $p+p \rightarrow d+\pi^+$ for pions with a center-of-mass energy of 78 Mev. Once the experimental data on the $p+d \rightarrow t+\pi^+$ process are available, the theoretical treatment can be reversed or modified

to give information on the estimates and assumptions used.

KINEMATICS

The incident particles in the process $p+d \rightarrow t+\pi^+$ are the 340-Mev protons from the Berkeley 184-inch synchrocyclotron. For such a monoenergetic two-body process, the conservation equations for energy and momentum can be solved to give the correlated angles and energies of the resultant particles; these angles and energies are summarized in Fig. 1. One important feature of this angular correlation curve is that the tritons are confined within a 12° cone about the beam axis. In the analogous reaction $p+p \rightarrow d+\pi^+$, the deuterons are confined to a 6° cone. The triton cone is larger because the extra target nucleon reduces the center-of-mass motion; thus the effect of the triton momentum component perpendicular to the beam axis is more pronounced. This reduced center-of-mass motion, for 340-Mev incident protons, makes 219 Mev available for a $p+d$ process compared to 163 Mev for a $p+p$ process. Thus, pion production takes a small enough bite of the 340-Mev input energy that pions and tritons are produced at angles and with energies adequate for a counter experiment.

The concentration of tritons within a small angular region in the forward direction makes possible a triton time-of-flight measurement without a sacrifice in counting rate. For example, consider the correlated angles of 8.0° for the triton and 110° for the pion. In this region of Fig. 1, a 9° center-of-mass angular interval for tritons is compressed into a 1° laboratory angular interval; in the same transformation, the pion angular interval is changed only slightly. If, then, the distance of the triton counters from the target is nine times that of the pion counters, the same center-of-mass polar angular interval will be subtended by triton and pion counters of equal horizontal dimensions. Also, even though the triton counters are considerably farther from the target than the pion counters, both sets of counters will be about the same perpendicular distance from the beam axis; therefore, triton and pion counters of roughly the same vertical dimensions

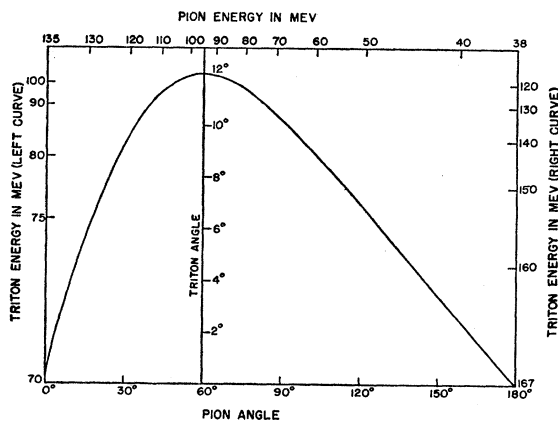


FIG. 1. Correlated angles and energies in the laboratory system for the process $p+d \rightarrow t+\pi^+$. The incident proton energy is 340 Mev.

* Now at the Brookhaven National Laboratory, Upton, New York.

¹ M. Ruderman, Phys. Rev. **87**, 383 (1952).

² A. M. L. Messiah, Phys. Rev. **86**, 430 (1952).

³ S. Bludman, following paper, Phys. Rev. **94**, 1722 (1954).

will intercept the same azimuthal interval. This fact is illustrated qualitatively in a scale drawing of the experiment arrangement in Fig. 2. In summary, the solid angle determined by the pion counters at a distance of 14 in. from the target is not reduced by placing similar-sized triton counters 11 ft from the target. This large triton-counter distance allows the triton time of flight to be measured.

EXPERIMENTAL APPARATUS

The experimental arrangement at a typical angle is illustrated in Fig. 2. The incident 340-Mev protons were collimated to a 2-in. diameter beam. The beam was monitored by an ionization chamber; the ion current was integrated on a calibrated condenser and recorded in units of volts by a recording millivoltmeter. The targets of deuterated paraffin (CD₂) and carbon (C) were 3 in. in diameter and contained the same number of carbon atoms. The particle detector at the triton angle consisted of two trans-stilbene phosphors; each phosphor was 2 in. by 4 in. and was viewed by two

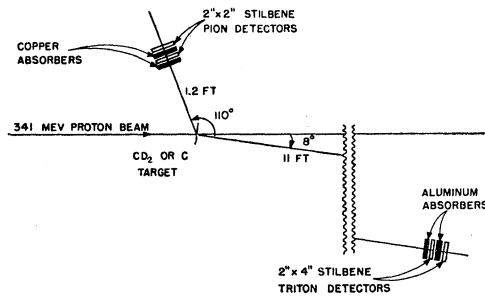


FIG. 2. Experimental arrangement for observing the process $p + d \rightarrow t + \pi^+$.

1P21 photomultiplier tubes. The phosphor thicknesses were selected so that the expected tritons, after suitable absorber, would lose 20 to 30 Mev in each phosphor. The two signals from a given counter were shaped by clipping to a width of 3 millimicroseconds and added together. Figure 3 shows this pulse shaping and adder circuit, together with the last dynode stage of the photomultiplier. The high impedance (259-ohm) coaxial cable was used to increase the signal transmitted from the photomultiplier and help eliminate the need for amplifiers between the photomultiplier and the coincidence circuit.

The particle detector at the pion angle consisted of two trans-stilbene phosphors; each phosphor was 2 in. square and was viewed by one 1P21 photomultiplier tube. The phosphor thicknesses were selected so that the expected pions, after suitable absorber, would lose 10 to 15 Mev in each. Each pion signal was clipped to a width of 3 millimicroseconds and delayed by a length of coaxial line calculated to match the expected triton-signal time of arrival at the coincidence circuit. The two triton signals and the two delayed pion signals

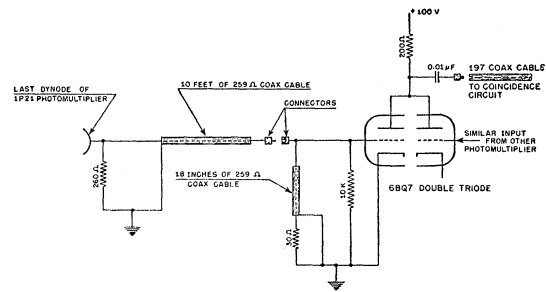


FIG. 3. Circuit used to shape, limit, and add photomultiplier pulses.

were fed into a germanium diode quadruple coincidence circuit.

Figure 4 is a schematic diagram of the coincidence circuit. The IN38 germanium diode inputs are used instead of vacuum tubes to increase the circuit sensitivity. The diode circuit can be driven directly from the output of the pulse-shaping circuit without the aid of distributed amplifiers. The three parallel IN56 diodes and the associated capacitor are due to Garwin.⁴ They increase the discrimination ratio by clamping the output voltage in all cases in which less than four of the input diodes are cut off. The IN54A diode in the grid of the output tube is introduced to increase further the discrimination of the circuit and, with the grid resistance, provide a pulse-lengthening action. The ratio of quadruple to triple coincidence output pulse heights is better than sixteen.

The output signal of the coincidence circuit is amplified and lengthened with a secondary emission tube (Phillips type EFP-60) and recorded on two scaling units. The discriminator for each scaler is calibrated so that the two different discriminator bias settings provide a measure of the bias plateau. If only one discriminator were used, the running time would be increased. The efficiency of the counting equipment has been measured to be almost 100 percent. The resolution time of the overall system is about 3 millimicroseconds. A more detailed account of the

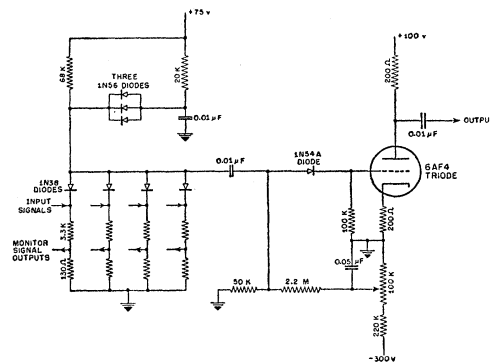


FIG. 4. Germanium diode quadruple coincidence circuit.

⁴ R. L. Garwin, Rev. Sci. Instr. 21, 569 (1950).

electronic equipment is being published by Richard Madey.

EXPERIMENTAL METHOD

Because the counting rates were on the order of one count a minute in this experiment, the process $p+d \rightarrow t+\pi^+$ was identified by a number of tests at only one angle; at each angle, however, three conditions were placed on the coincidences observed: (1) the counters were set at a given pair of correlated angles; (2) a time-of-flight requirement was placed on the triton by delaying the pion signals relative to the triton signals according to the calculated relative velocities; (3) the absorbers added to each counter telescope were selected to stop any particles with ranges below the minimum calculated ranges.

The 340-Mev scattered deflected external proton beam⁵ pulses from the Berkeley cyclotron have envelopes of roughly 25 microseconds duration. The pulse repetition rate is about 60 per second. Within this pulse envelope, a fine structure exists with the 16-Mc frequency of a phase-stable bunch of protons circulating near the machine's maximum radius. Thus, the fine-structure interval between proton pulses is 60 millimicroseconds; the width at half-maximum of a single pulse of protons is 4 millimicroseconds.⁶ The bunched protons in the beam produce bunched background processes in the target that have cross sections several orders of magnitude larger than the cross section of the process $p+d \rightarrow t+\pi^+$; however, the time-of-flight method used for measuring the triton velocity also separates background processes by means of their different velocities.

The time-of-flight method will discriminate only against background particles with velocities different enough from the expected triton velocity to separate the two particles at the triton counter by a time comparable to the resolution time of the coincidence circuit. However, background particles with the same velocity as the triton can be absorbed out if their masses are less than the triton mass. For example, protons and deuterons have respectively one-third and two-thirds the range of tritons of the same velocity. By adding enough absorber before a counter telescope to stop the expected particle at the back of the last phosphor, most background particles with velocities similar to the expected triton velocity can be eliminated.

The calculations for a typical angle will be used to illustrate the method more specifically. For the case of a pion center-of-mass angle at 130° , the laboratory correlated angles are 8.0° for the triton and 110° for the pion. The triton energies are double-valued, but the pion angle requirement eliminates one possibility.

⁵ C. E. Leith, Phys. Rev. 78, 89 (1950).

⁶ Madey, Bandtel, and Frank (unpublished measurements). For the method, compare "The Radiofrequency Fine Structure of the Photon Beam from the Berkeley Synchrotron" to be published in the *Review of Scientific Instruments* by the same authors.

The geometry is shown in Fig. 2. Suppose a time origin is taken when a proton pulse passes through the target. Assume that a triton-pion pair or a miscellaneous pair of background particles is created at some time within a radiofrequency proton beam pulse. The triton and pion are created simultaneously, but the background particles occur separately, spaced at most by the width of the radiofrequency envelope. (This condition is somewhat idealized, but most of the background trouble might be expected and was found to arise from the many protons in the peak of the radiofrequency beam pulse rather than from the few protons in the trough between pulses.) The pion velocity at 110° is 69 percent of the velocity of light, or 0.69c; the pion arrives at its counter in two millimicroseconds. The pion-counter background travels more slowly, except for electron and gamma rays, but is not debunched much over the short distance from the target to the counters. The time sequence of events being described is illustrated in Fig. 5. The triton velocity at 8.0° is 0.31c, while the velocity of elastically scattered protons is about 0.67c. Over the 11 ft from the target to the counters, the production probability envelopes of these two particles become separated by about 20 millimicroseconds. If the pion counter signals are delayed with an amount of delay line calculated from the pion-triton expected time of flight, the real pion-triton counts are placed in coincidence. The pion-counter background is well separated from the fast background at the triton counter; possible accidental coincidences are further discriminated against by the 3 millimicroseconds resolving time of the coincidence equipment.

Absorbers calculated to stop the expected particle at the back of the last phosphor were added to each counter telescope; the larger pulse height obtained from the expected particle's increased energy loss in the phosphor allows less energy-loss background to be biased out. The aluminum absorber calculated for tritons at 8.0° will stop 85-Mev protons. Figure 5 shows that protons of this energy and greater are in the fast-background category and are discriminated against by the coincidence-circuit resolving time.

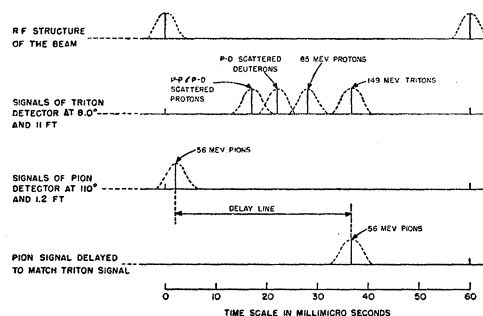


Fig. 5. Time sequence of particles arriving at the counters. The time origin is taken as the arrival of a single radiofrequency proton pulse at the target.

In summary, the method is this: two particles are detected in coincidence at angles correlated for the process $p + d \rightarrow t + \pi^+$; greater-velocity background is eliminated by a time-of-flight requirement; similar-velocity background is eliminated by a range requirement. The success of the method is seen in the fact that a CD_2 -to-C ratio of 5:1 was obtained at most angles without using unreasonably low beam intensities.

EXPERIMENTAL RESULTS

Identification

When the method described above was first developed, a number of identification tests were made at one angle in order to be certain that the process $p + d \rightarrow t + \pi^+$ was really being observed. The correlated angles of 8.0° for the triton and 110° for the pion were chosen at that time for two reasons. First, since pion production from nucleon-nucleon collisions typically has an $(a + b \cos^2\theta)$ -type of angular distribution, pion angles away from 90° in the center-of-mass system or 70° in the laboratory system were to be preferred in order to utilize the possibly higher cross section. Second, since the cross section for $p + d \rightarrow t + \pi^+$ might

TABLE I. CD_2 -C difference counting rate as a function of relative beam intensity. The rate units are counts per unit of integrated beam.

Relative beam intensity	CD_2 -C difference rate	Approximate CD_2 -to-C ratio
6	1.00 ± 0.20	3:1
1	1.25 ± 0.30	6:1

be one or two orders of magnitude lower than the $p + p \rightarrow d + \pi^+$ process, accidental coincidences could be expected to be one of the major experimental difficulties. This source of trouble could be reduced by selecting a pion angle in the back quadrant correlated with a large triton angle. Unfortunately, the largest triton angle in the laboratory system is in the region of 90° in the center-of-mass system. The correlated angles for the identification test were chosen as a compromise between a possible low real counting rate and a possible high accidental counting rate. As it turned out, this pair of angles was among the most difficult at which data were obtained.

As the first step, a difference in the coincidence counting rates from CD_2 and C targets was obtained, with the calculated absorbers and delay lines, at the correlated laboratory angles of 8.0° for the triton and 110° for the pion. The result of varying the proton beam intensity is given in Table I. The target-out counting rate was a factor of five below the carbon rate at the higher intensity. The fact that the difference counting rate was constant over a large variation in intensity indicates that a real process from protons on deuterons was being observed. The identification tests

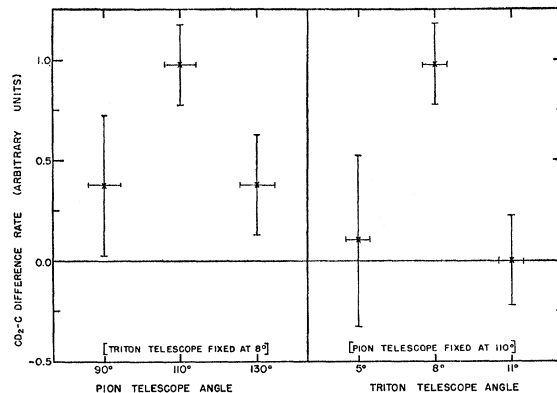


Fig. 6. Angular correlation test for the process $p + d \rightarrow t + \pi^+$. The correlated angles are 8° for the triton and 110° for the pion.

for this real process were made by changing the angles, absorbers, and delay lines from the calculated values and observing the reduction in the difference counting rate.

The angular correlation of the process was tested by moving each counter telescope separately from its calculated angle. The results, plotted in Fig. 6, show that the difference was properly reduced in each case. The large amount of triton multiple scattering and the fact that the pion counters were moved only two counter widths to each side while the triton counters were changed by three counter widths account for the incomplete disappearance of the counting rate in the pion-angle correlation test. The coplanarity of the process was tested by raising the triton counters one counter height out of the plane formed by the beam axis and the pion counters; the difference rate dropped to 0.00 ± 0.30 from the normal 1.00 ± 0.20 counts per integrated beam unit.

The time-of-flight correlation of the process was tested by changing the arrival time of the pion signal relative to the triton signal. The results of varying the length of pion delay line are given in Fig. 7. The difference counting rate is a maximum when the length of delay line in the pion counters is chosen to match the expected triton velocity; the difference rate disappears for particle velocities larger or smaller by 12 percent. The effectiveness of the time-of-flight and range methods in reducing background counts may be appreciated by noting how rapidly the carbon counting rate rises as delay is removed between the pion counters and the coincidence circuit. The reason for the rise in this accidental coincidence rate can be understood from Fig. 5; the shorter delay allows the pion-counter background to synchronize with the faster triton-counter background.

The ranges of the particles causing the coincidences were measured. The range spectrum of triton-counter particles participating in coincidences is shown in Fig. 8; the calculated triton ranges are indicated for comparison. The spread in the expected ranges is

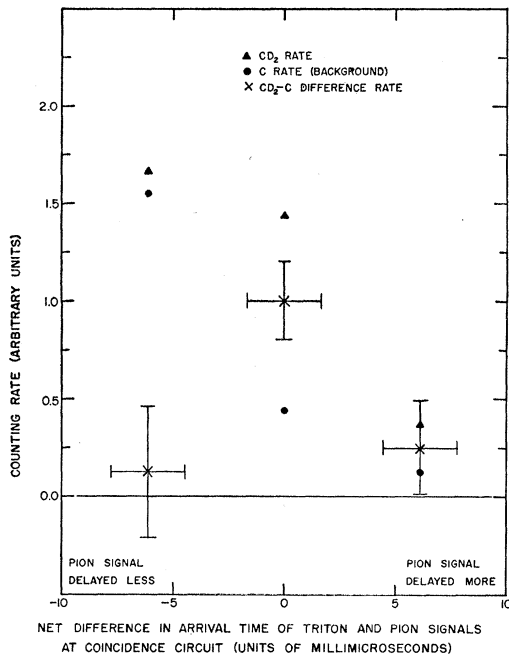


Fig. 7. Time correlation test for the process $p+d \rightarrow t+\pi^+$. Zero time is based on pion and triton calculated times of flight.

caused by production at different target depths. The measured range agrees with the calculated triton energy to within 10 percent. The effectiveness of the range method in reducing accidental coincidences due to similar-velocity background is illustrated by the fact that the CD_2 -to-C ratio of 3:1 with the absorber drops to 4:3 without the absorber. The range of pion-counter particles participating in coincidences was measured by adding more absorber to the pion counters; the measured range agrees with the predicted pion energy to within 10 percent.

When CH_2 was substituted for C, the CD_2-CH_2 difference remained the same as the CD_2-C difference. Thus, all these identification tests show a real process from protons on deuterons. This process is a mono-

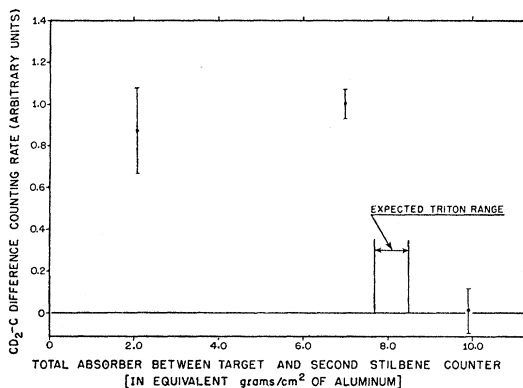


Fig. 8. Range spectrum of particles arriving at the triton counters, and causing a coincidence.

energetic two-body reaction that is consistent with the process $p+d \rightarrow t+\pi^+$. Because of the low counting rates in this experiment, such a series of tests could not be made for each angle without excessive use of cyclotron time. The general method of imposing the conditions of correlated angles, expected triton time of flight, and minimum ranges for both particles was extended to the other angles at which cross sections were obtained; however, no further tests were made.

Angular Distribution

Seven laboratory angles, corresponding to equally spaced center-of-mass angles, were chosen for the angular distribution; one of the middle angles, however, was omitted because of data-taking time limitations. The data were originally obtained in terms of counts per unit of integrated beam, but for interest are listed in Table II in terms of counts per minute. Three corrections were made to the data: (a) pion loss by decay in flight; (b) pion loss by absorption in the copper absorbers defining the minimum range; (c) triton loss and—to a lesser extent—pion loss by multiple scattering in the target.

TABLE II. The various counting rates (in units of counts/minute) as a function of pion center-of-mass angle.

Pion center-of-mass angle	CD_2 rate	C rate	CD_2/C ratio	CD_2-C difference rate
30	0.420	0.075	6	0.345 ± 0.085
50	0.985	0.095	10	0.890 ± 0.060
70	0.640	0.070	9	0.570 ± 0.080
90	0.990	0.065	15	0.925 ± 0.100
130	3.23	0.85	4	2.38 ± 0.31
150	0.700	0.360	2	0.340 ± 0.093

In the present experiment, the pion is detected only as a charged particle satisfying certain correlated angle, minimum-range, and time-of-flight requirements. Its muon decay product is charged and can produce a coincidence if it meets these requirements. Only about one-quarter of the muons can cause coincidences; even so, the pion decay correction never amounts to more than 5 percent because of the short pion flight path.

Because of the minimum range requirement placed on the pion, the pion passes through an appreciable amount of copper absorber before being detected. Some of the pions interact with the copper nuclei and are absorbed, or scattered at large angles. The recent data of Stork⁷ at this laboratory on π^+ absorption in copper was plotted in the form of the absorption coefficient, μ , versus the absorber thickness, t , in radiation lengths; the integral $\int_{t_1}^{t_2} \mu dt$ was evaluated numerically over the absorber thickness to give the correction factor, $\exp \int_{t_1}^{t_2} \mu dt$. This factor increases with the pion energy, and at most, amounts to 1.40, corresponding to a 30 percent pion loss. If this correction

⁷ D. Stork (private communication).

were avoided by removing the minimum range requirement, the higher accidental coincidence rate and consequently the lower CD_2 -to-C ratio would increase the data-taking time requirements severalfold and make the experiment unfeasible from the standpoint of available cyclotron time.

In passing through the target and the eleven feet of air between the target and the counter system, the triton undergoes multiple scattering which sometimes destroys the angular correlation with its paired pion. Ordinarily this loss would be avoided by making the triton counters large enough to intercept all the scattered particles, while allowing the pion counters to define the solid angle. There are several difficulties with such a procedure in the present experiment. In order to identify the process and suppress the background, a long time-of-flight path is required for the triton; even so, equal-sized pion and triton counters subtend approximately the same center-of-mass solid angle. To eliminate a multiple-scattering correction, the pion counter must be reduced in size or the triton counter extended in size. The change should be by at least a factor of two in linear dimensions, or a factor

TABLE III. Correction factors and differential cross sections at various pion center-of-mass angles for the process $p + d \rightarrow t + \pi^+$.

Pion center-of-mass angle	Total correction factor	$d\sigma/d\Omega_0$ (microbarns/steradian)
30	1.94	3.95 ± 0.97
50	2.21	2.55 ± 0.18
70	2.24	0.77 ± 0.11
90	2.21	0.44 ± 0.05
130	1.82	0.46 ± 0.07
150	1.66	0.41 ± 0.12

of four in area. If the pion counters are made smaller, the already marginal counting rate becomes unreasonably low. Larger triton counters are difficult to make with a uniform detection efficiency for short resolution time and short deadtime coincidence counting; moreover, this extra area represents a fourfold increase in the accidental counting rate, but a less than double increase in the real counting rate. A further complication is provided by the double-valued angular correlation curve if the same counters are used at all the desired data-taking angles. In the actual experimental arrangement, the solid angle was determined by the pion counter while the triton counter usually subtended a somewhat larger area. The correction factor for scattering loss is about 1.80 at 90° (pion center-of-mass angle) and falls to around 1.50 at 30° and 150° . The total correction factors applied to the data, as well as the final differential cross sections, are given in Table III. The errors shown are the statistical standard

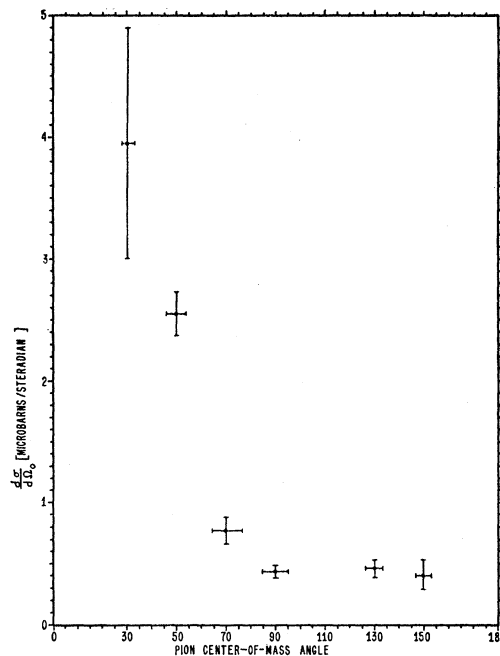


FIG. 9. Experimental angular distribution for the process $p + d \rightarrow t + \pi^+$.

deviations related to the number of counts in the original data.

The angular distribution data have been plotted in Fig. 9. If a reasonably smooth curve is drawn through the points, the total cross section is estimated by numerical integration to be 15 microbarns. The total error in the integrated number of protons, the target particle density, and the solid angle subtended is estimated to be 10 percent. Since the counting equipment is nearly 100 percent efficient, this cross section can be taken as the absolute yield within 25 percent.

CONCLUSIONS

The most noticeable feature of the $p + d \rightarrow t + \pi^+$ angular distribution is the constant cross section part from 90° to 180° . Ruderman's theoretical distribution,¹ derived in terms of the $p + p \rightarrow d + \pi^+$ experimental distribution by using an impulse approximation method, has a 90° minimum with a large 0° peak, and a lesser 180° peak. In reconsidering the problem, Bludman² has been able to fit the experimental data quite well by introducing Jastrow's nucleon model³ of a short-range repulsive force surrounded by the usual longer-range attractive force. A comparison of the theoretical and experimental results is given in the following article.

¹ R. Jastrow, Phys. Rev. **81**, 165 (1951).